Adv. Space Res. Vol.4, No.7, pp.163-174, 1984
Printed in Great Britain.

0273-1177/84 $0.00 + .50

CORONAL MASS-EJECTION EVENTS

Richard R. Fisher

High-Altitude Observatory, National Center for Atmospheric Research, P.O. Box 3000, Boulder, CO 80307, U.S.A.

ABSTRACT

Nearly fifteen years have passed since the discovery of coronal mass ejection events from the solar atmosphere. Progress in the interpretation of the observational results has led to a body of knowledge concerning the geometrical and evolutionary properties, physical characteristics, and the association of this type of event with other forms of solar activity. Recent interpretive results taken from the large body of observational data now available are discussed below in some detail. A classification system based on kinetic properties of these events is presented.

INTRODUCTION

Reviewing a sequence of daily observations of the lower solar corona made with a ground-based K-coronameter, Hansen, et al. /1/ concluded that significant amounts of coronal material were depleted from the lower solar atmosphere between daily observations. Not accounted for by the simple effect of solar rotation of coronal structures, it appeared that, upon occasion, a sudden depletion of the white light corona was observed in association with flare activity seen at the limb of the sun. With the subsequent development of orbital coronagraphs, having improved spatial and temporal resolution, it was quickly learned that sporadic mass ejection from the solar corona occurs with some regularity. Descriptions of these early observations with externally occulted satellite coronagraphs are given by Tousey /2/ and MacQueen, et al. /3/.

At the present time, coronal observations are made using both the ground-based K-coronameter technique (see Fisher, et al. /4/), and satellite instruments such as the NRL P-78 coronagraph (Sheeley et al. /5/) and the recently repaired SMM instrument (MacQueen, et al. /6/). Clearly it is now the case that the observational technique required for the detection of mass ejection events from the corona is mature and well understood; the efforts to interpret the body of data gathered continue with recent new developments. MacQueen /7/ and Wagner /8/ have given recent reviews of the observational material and its interpretation; it is the goal of this paper to discuss results unavailable to these authors.

Generally speaking, a coronal mass ejection event (CME) occurs when sufficient energy is supplied to the corona to cause some substantial, and relatively coherent, mass to be removed from the gravitational potential well of the sun and sent irreversibly into motion outward into the interplanetary region of the solar system. This is distinctly different from transient changes in the morphology of the corona which occur on the time scales of many hours but for which the net mass of the corona remains unchanged to the first order. Investigators tend to visualize CME events as arch- or loop-like structures seen against the plane of the sky, and it is worth recalling the quoted fraction of all coronal transients which have this characteristic shape. During the 1973-1974 ATM epoch only about one-third of all the coronal transient events observed had an arch-like appearance, a result reported by MacQueen /9/. Using data obtained over the span 1979-1981, Sheeley, et al. /10/ found that one-half of all transients observed above 2.5 $R_\odot$ were characterized by the arch- or loop-like structure during this period near the maximum of the sunspot cycle. Considering only the CME events observed by the SMM coronagraph/polarimeter, Wagner /8/ found that the majority of such events, in excess of 80%, were characterized by the arch-like shape. Reviewing the data obtained from K-coronameter observations over the period 1980-1984, tabulated by Rock, et al. /11/, a similar fraction of mass depletion transients observed in the lower solar corona were characterized by this distinctive shape.

It is likely that a detection threshold definition, as well as observational selection effects, play important roles in the determination of the results quoted above. The typical shape is an image which has lingered with solar astronomers, characteristic of catastrophic mass loss from the corona. An example is shown in Figure 1.

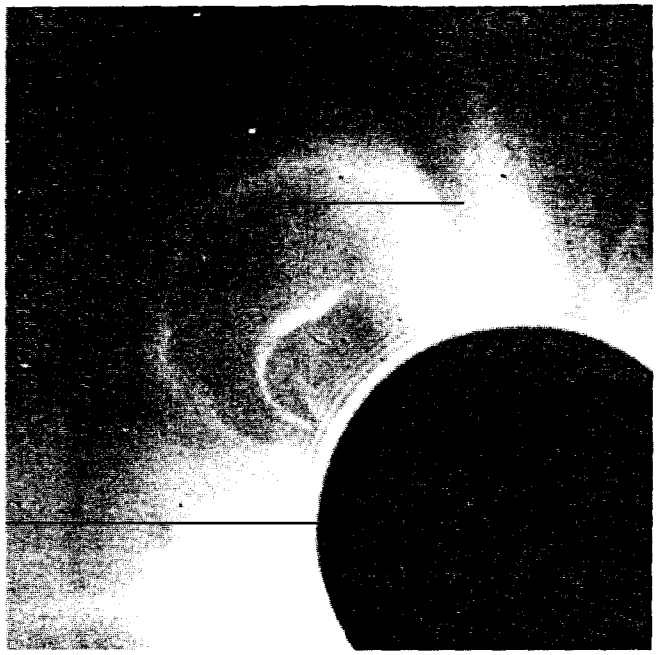

Fig. 1. The CME event of 14 April 1980, obtained with the coronagraph/polarimeter on the Solar Maximum Mission spacecraft (High Altitude Observatory, National Center for Atmospheric Research, Boulder, Colorado U.S.A.).

MORPHOLOGY, KINEMATICS, AND GEOMETRY

Since it is the case that the majority of CME events are seen as arch-like structures, at least in the lower corona from 1.2 to 4.0 $R_\odot$, we begin with a general description of the morphology. The initial appearance of the CME is usually a bright leading arch moving upward away from the occulting disk of the instrument in use. Following this leading bright arch, which is usually well developed by the time that the edge reaches a height of 1.8 $R_\odot$, is a region of depleted density. On occasion, usually associated with eruptive prominence events, the bright leading arch does not fully develop into a continuous structure until after reaching an altitude in excess of 1.5 $R_\odot$. When this occurs, the transient has the general appearance as a moving rarefaction outlined by density enhancements at the sides of the event. If an image differencing technique is used to detect such an event, the disturbance is seen as a moving depletion, giving rise to the term "dark transient." As the CME continues outward into the interplanetary medium, the leading arch brightens and then the leading arch tends to fade again, leaving two legs connected back down to the photosphere. In the late stages of the CME event, after the leading edge has either faded or passed out of the coronagraph field of view, the bright legs frequently outline the path of the CME and delineate the volume of the corona depleted by the event.

Within the depleted region found behind the leading bright arch, enhanced regions are sometimes included. CME events which are associated with eruptive prominences frequently enclose bright $H\alpha$ prominence material. This material appears brighter than the surrounding depleted region and may be caused either by the scattering of chromospheric $H\alpha$ by neutral hydrogen, or by scattering of photospheric white light by electrons obtained from ionization of the prominence material. Another kind of structure occasionally found within the depleted volume is a second (or third) bright arch, giving rise to the so-called filled bottle type of event.

Another part of transient morphology is the so-called mass forerunner, a region of enhanced coronal density extending outward from the front of the initial bright arch to the point where there is no detectable enhancement with respect to the pre-event coronal structure. Such a feature was found leading twenty-one CME events observed with the ATM coronagraph by Jackson and Hildner /12/; only one such feature has been reported by Wagner /8/ in the investigation of CME events in the SMM data set. No forerunner has ever been detected in the K-coronameter data although this may be accounted for by a consideration of signal to noise characteristics. Jackson and Hildner /12/ concluded that only about 10 to 15% of the CME mass was involved in the forerunner structure, a fraction of mass too small for reliable detection by the coronameter system at Mauna Loa.

This description of CME appearance is a composite one, built up from several different kinds of observations, and not every CME event detected exhibits all of the characteristics outlined above. The description of transient behavior in the lower corona (1.2 -2.2 $R_\odot$) is obtained from K-coronameter results given by Fisher and Poland /13/, and Fisher, et al. /14/. Descriptions of CME events detected at heights above 2.0 $R_\odot$ have been given for the ATM, 1973-1974 epoch, by Hildner /15/ and for periods near the maximum of solar cycle 21 by House et al. /16/, and Sheeley, et al. /17/.

The kinematic properties of CME events are relatively well understood, since only the plane of the sky speed need to be measured. At low altitude levels in the corona, 1.2 to 1.5 $R_\odot$, the radial and lateral speeds of CME events tend to be approximately equal in the early phase of the event. By the time the leading edge of the CME reaches a height of a fraction of a solar radius, lateral acceleration falls to nearly zero and the lateral extent of the lowest observable portion of the transient tends to remain more or less fixed for the remainder of the event lifetime. Gosling, et al. /18/ found that the range of speeds detected above 2.5 $R_\odot$ ranged from 100 km sec^{-1} to 1100 km sec^{-1}, with an average outward speed of about 500 km sec^{-1}. In a study of selected K-coronameter events, MacQueen and Fisher /19/ found values for the lateral speed at the transient base and radial velocity as a function of height. These are summarized in Figures 2 and 3.

Figure 3 illustrates the point that there is a clear distinction to be made in the acceleration history of a CME event depending upon the type of H_α event associated with the corona disturbance. Flare associated events (marked with an "F") tend to show little or no evidence of acceleration between 1.2 and 2.2 $R_\odot$, and they tend to have higher speeds measured in the plane of the sky. Those CME events associated with eruptive prominences (and no flare) exhibit acceleration through the lower corona. This point was initially masked by the externally occulted coronagraphs since the typical field of view tends to be limited to heights of greater than 2.0 $R_\odot$.

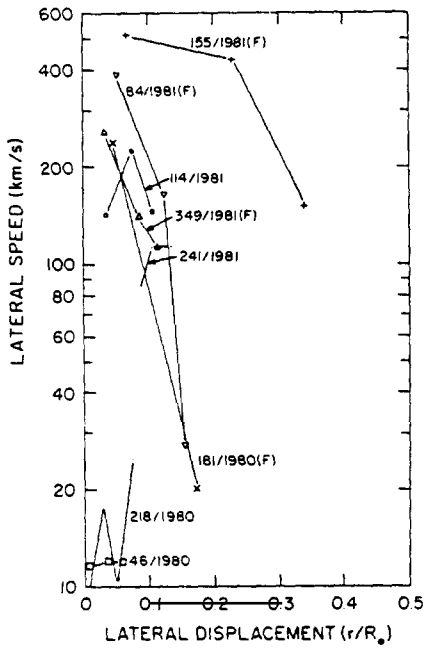

Fig. 2. The lateral speed of CME transient leg separation measured at a height of 1.2 $R_\odot$ as a function of leg displacement tangent to the limb (MacQueen and Fisher /19/).

Finally a third kinematic distinction may be made. There are observations of CME events having rather having slow, 10-40 km sec-1, eruption speeds; these are not associated with either chromospheric flares or erupting prominences. Several such events in the lower solar corona are described by Garcia, Fisher and MacQueen /20/. The reason for the relatively few recognitions of such events seems to hinge on the ability to perceive change over the time scale of a typical observation period. These events require a large fraction of a day in order to evolve, and the speeds encountered in the initial phases of the event are substantially lower than the inferred local sound speed estimated for ambient coronal conditions. A typical white light slow transient is described by Fisher and Garcia /21/. Another interesting feature of this event was reported by Altrock and Demastus /22/ who detected enhanced Fe XIV

emission consistent with the site of a slow transient. Emission line transients generally seem to be poorly correlated with CMEs, and the detection of Fe XIV associated with a slow event indicates the presence of a considerable fraction of the CME mass was at a relatively elevated temperature, logT = 6.30. For this class of CME, the driving forces operate on large scale coronal structures for many hours, if not days.

To date, it has not been possible to identify a kinematic property of CME events which allows the unambiguous identification of a physical effect driving for a given event. MacQueen and Fisher /19/ concluded that the radial acceleration history of eruptive prominence associated CMEs was consistent with the pressure gradient forces expected for the acceleration of the solar wind in the lower corona below the critical point. Flare associated events, which show little acceleration at heights greater than 1.2 $R_\odot$, evidently are generated by forces which act for a rather brief time. These events may be the result of an impulsive input of energy which operates for a time short compared to that required for the transit of the CME from the site of origination to the lower limit of the K-III coronameter field of view.

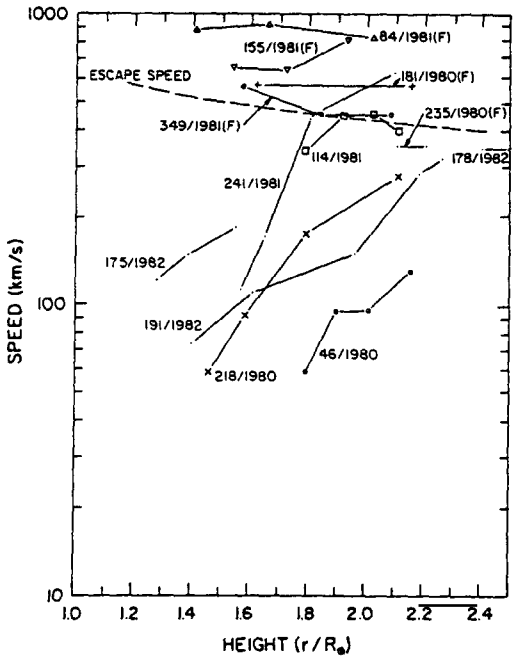

Fig. 3. Radial speeds of 12 CME events as a function of height (MacQueen and Fisher /19/).

Masses associated with CME events are estimated using assumptions about the distribution along the line of sight. If it is assumed that all of the excess mass visualized in a CME event is constrained to the plane of the sky, then an upper limit may be obtained by scaling the excess brightness using a simplified Thomson scattering model (see Billings /23/). A review of mass estimates of CME events observed with the ATM coronagraph is given by Rust, et al. /24/ who found that this simplified technique gives a range of flare-associated and epl-associated CME masses between 8×10^{14} up to 2×10^{16} grams. A single estimate of mass for the case of a slow transient was given by Fisher and Garcia /21/. They found that 2×10^{14} grams of material was injected into the field of view from beneath the occulting disk, and after the event left the field of view, the net coronal depletion was about ten times this value.

A refinement in this method for the estimation of CME mass depends upon the distribution of material over three dimensions. This confronts the investigator with the question of CME geometry and event location with respect to the plane of the sky. Since the white light corona is optically thin, the observed brightness, or polarized brightness, at any given point above the limb is equal to the integral of the product of the density and the efficiency of scattering of photospheric light over the observer's line of sight. The theory of this process is given by van de Hulst /25/. It was recognized by Fisher and Munro /26/ that the depleted regions of CMEs could be used to estimate a minimum necessary path length required to produced the observed reduction in coronal polarized brightness found behind the bright leading edge of a mass ejection event, if one assumed an absolutely perfect depletion to zero electron density. This estimated lower limit to the path length is an indication of the thickness of the depleted volume normal to the plane of the sky, and does not depend upon the specific distribution of electron density. Estimates of the contrast of depleted regions

of a number of CME events seen at Mauna Loa with the K-coronameter, which measures coronal polarized brightness, routinely yield estimates of 0.3 $R_\odot$ to 0.6 $R_\odot$ for the typical minimum thickness of the depleted region normal to the plane of the sky.

The only attempt at the inversion of the distribution of brightness and polarized brightness of a coronal mass ejection yielded a report of a bubble-shaped transient geometry in an analysis by Crifo, et al. /27/. In a separate study of a flare-associated CME originating near the limb, Fisher and Munro /26/ found that a structure with cylindrical symmetry could be used to make a self-consistent electron density model, which then could be used to refine estimates of the change in total coronal mass during this event. A schematic representation of the CME at a leading edge height of about 2.0 $R_\odot$ is shown in Figure 4. The result obtained from this model indicated that about 2 x 10^{15} grams of material was injected into the field of view (1.2 - 2.2 $R_\odot$) and that after the event had passed beyond the upper limit of the field of view, a net decrease of 2 x 10^{15} grams had occurred with respect to the pre-event value found for total coronal mass. This implies that about half of the total change of mass was supplied by the pre-event corona, the other half originated at heights lower than the limit of the occulting disk. This is consistent with total mass estimates obtained from ATM data and summarized by MacQueen /9/. Finally, the NRL P-78 coronagraph has observed a flare associated CME which evidently was directed, more or less, at the earth, originating from a point near the center of the solar disk. This was visualized as a bright halo seen around the coronagraph occulting disk. This event, reported by Howard, et al. /28/, has two possible interpretations; it could have been either cone shaped with a filled interior, or a conical shell with an optically thin leading front. There seems to be little doubt that at least some CME events are three dimensional in nature, even though they have an arch- or loop-like structure viewed against the plane of the sky; the depleted regions could result from removing coronal material from within either a bubble-shaped disturbance or a long arcade of loop structures.

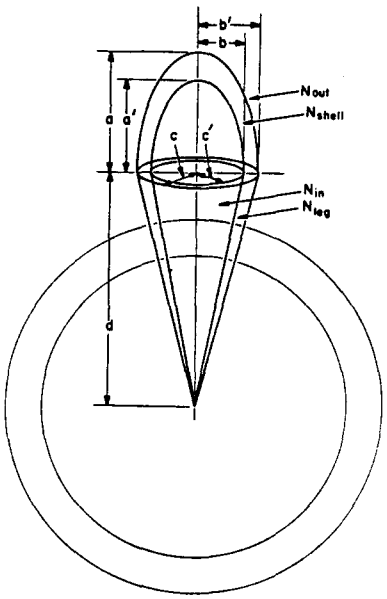

Fig. 4. The schematic of a CME model having the necessary geometric and density parameters required to reproduce the observed polarized brightness distribution.

N_{out} = 1.35, N_{shell} = N_{leg} = 4.0, and N_{in} = 0.0, where the unit of density is the value of the Saito Quiet Coronal Background density 1.8 x 108 electrons cm^{-3}, (Fisher and Munro /26/) and the event is assumed to have occurred at the limb.

The question of CME geometry remains an important one, and no systematic analysis of the distribution of polarization and intensity (or alternatively polarized brightness) has been attempted for a large set of CME data. Lacking this sort of analysis on some substantial number of events, it is impossible to make any general statements concerning the assumption of either bubble or loop geometries in the calculation of physical CME models.

Having measured the plane of the sky speeds and estimated mass from simple scattering theory, it is possible to estimate CME kinetic energy. Assuming that the average CME velocity is of

the order of 500 km sec, and that an average mass is 4×10^{15} grams, the kinetic energy of this hypothetical event is 5×10^{31} ergs, a number frequently found in the literature as a estimate typical for CMEs. However, the range of energies inferred actually spans from the value of 10^{27} ergs to 10^{32} ergs, depending more upon the kinematic properties than variations in mass.

FREQUENCY, LATITUDE DISTRIBUTION AND ASSOCIATION WITH SURFACE ACTIVITY

The rate of occurrence of CME events depends crucially upon the definition of CME and threshold adopted for the recognition of a specific event. Using direct images from the ATM data set (1973 - 1974), Hildner, et al. /30/ were able to show that the rate of production of CMEs was not constant through the period of observation. They suggested that the variation in rate was related to a familiar index of solar magnetic activity, the sunspot number, and conjectured that the rate of transient production would be somewhat higher at the time of solar maximum. Using the images obtained in 1980, near the time of the maximum of sunspot cycle 21, Hundhausen et. al /31/ found that, contrary to expectation, the rate of transient production was approximately the same as that previously determined. It should be remembered that the sunspot number and flare production rate increased from 1973 to 1980 by factors of five and six respectively. The estimates obtained by Hundhausen, et al. /31/ were corrected for the effects of the sizes of the instrument's fields of view and data rates, and on the basis of more than one image per orbit, the CME rate near solar minimum (ATM, 1973-1974) was found to be 0.74 per day, while the value near solar maximum (SMM, 1980) was close to 0.87 per day. Effects of different sampling assumptions might modify these values by as much as a factor of two. It is not surprising that the transient rate estimated by Sheeley /32/ from the NRL P-78 data obtained in 1979-1981 is somewhat larger, nearly two events per day. The technique used in data reduction by this author, image differencing, is more sensitive and results in a lower detection threshold. It seems clear that while there is some uncertainty about the absolute rate of CME occurrence, the relative rate of CME production does not exhibit strong modulation over the sunspot cycle.

A quantity that apparently is variable over the activity cycle is the projected latitude of the CME transient origin. Considering the fraction of transients produced in a latitude bands fifteen degrees in width, Munro, et al. /33/ found that near solar minimum, transients rarely originate from latitudes higher than N45 or lower than S45. Hundhausen, et al. /31/ constructed the same type of diagram for the SMM data taken in 1980, and noted that the distribution of fraction of CMEs per fifteen degree latitude band was much broader and less peaked at the equator. The difference between these two diagrams, after being carefully corrected to eliminate differences in instrument performance and sampling, caused the above authors to conclude that a larger fraction of CME events occur at high solar latitudes during the maximum phase of the activity cycle. These two diagrams are plotted in Figure 5.

Munro, et al., /33/ attempted to associate the set of CME events observed in 1973-1974 with the observed surface activity events. They concluded that there is a strong correlation between CMEs and $H\alpha$ activity. About one-half of all CME events were associated with ejected $H\alpha$ material, eruptive prominences without flare activity, and flares. Of those events which

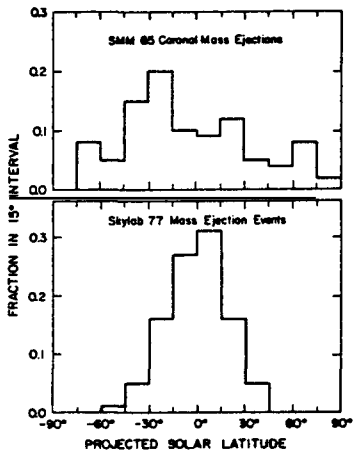

Fig. 5. The projected solar latitudes of coronal mass ejections. The top frame shows the distribution of projected latitudes for the 65 SMM mass ejections (Hundhausen, et al. /31/). The bottom frame shows the distribution for 77 mass ejection events observed during the Skylab Mission (Munro, et al. /33/).

could be associated with near surface activity, 40% of the CMEs were associated with flares and 50 % were associated with eruptive prominences or filament disappearances without concurrent flares.

The association study indicates that some CME events are associated with the magnetic evolution of active regions. By separating X-ray flare images into two classes, Pallavicini, et al. /34/ were able to find a strong positive correlation between long duration X-ray events (greater than 3 hours) in diffuse loop arcade systems and CME events. Using the same set of transients investigated by MacQueen and Fisher /19/, Fisher /35/ was able to define a "probable location" box, five degrees extent in latitude and twenty five degrees of longitude in width, and fix this site with respect to a synoptic observation of the longitudinal magnetic field in the photosphere. In eleven of twelve cases, the CME site of probable origin contained a region in which the sign of the inferred longitudinal photospheric field changed sign. In six of these cases, epl-associated transients were associated with non-active region, large scale neutral line features in the photospheric magnetic field. This is consistent with the observation that filaments on the disk tend to lie between regions of opposite polarity and with the strong association between eruptive prominences and CMEs. Hildner /15/ previously suggested that CMEs are generated through some mechanism of field evolution at the boundaries of large scale magnetic regions identified with photospheric observations. A recent review of transients detected in the SMM data set by Illing and Hundhausen /36/ suggests that there is observational evidence of magnetic field reconnection at the trailing edge of a CME. Namely, the discovery of an arch-like structure, concave with respect to the limb, which moves outward, apparently at the trailing edge of a transient.

One of the interesting points that has come to light during the recent SMM observing period in 1980 is the relationship between CMEs and flare blast shocks. Simultaneous observations with the coronagraph and radioheliographs operating at 160, 80 and 43 MHz, have allowed investigators such as Wagner /37/, Gary, et al. /38/, Stewart, et al. /39/, and Gergely, et al. /40/, to fix the location of radio sources as a function of time for type II radio events occurring at the time of CMEs. These authors note the lack of spatial coincidence between the leading edge of this CME and the radio source. Wagner and MacQueen /41/ were led to propose that some flare associated type II bursts may originate from the interaction between a shock wave and the legs of a transient. Wagner /42/ reviewed the onset times of five type II events, and noted that the CME inferred launch time, subject to some uncertainty, for the coronal events tended to occur several minutes before the radio emission flare shock. For these two reasons, he concluded that the radio emission from type II events, believed to originate from flare blast shocks, were events separate from the CME structure. This is in contrast with the suggestion of Maxwell and Dryer /43/, and others, based on swept frequency interferometer data, that blast shock was leading or coincident with the CME leading bright arch. The effects of ionospheric refraction in the earth's atmosphere may confuse the identification of the position of the radio source.

Kahler and Cliver /44/ reviewed the available data for CME events associated with metric type II bursts, and they concluded that the evidence tends to support the hypotheses that CME structures and shocks are in many cases. They also found that there is a strong correlation between the speed of the CME and the onset of a type II burst. Conversely, Sheeley, et al. /45/ concluded that there are occasions when fast CME events are generated in association with flares and enhanced X-ray emission in the 1-8 A region, but for which no type-II burst is observable.

In a review of the relationship between CME events, type II metric bursts, and interplanetary shocks, Cane /46/ concluded that the reported observations of these phenomena are most easily interpreted by the adoption of a model in which coronal type II events are generated when a shock wave traveling at 1000 km sec^{-1} overtakes a slower moving CME structure with enhanced density.

INTERPLANETARY MANIFESTATIONS

Derived from simple models of electron scattering, inferred mass estimates of CMEs range over values of 2×10^{14} to 10^{16}, as was mentioned above. The inferred speeds of transients, estimated from plane of the sky measurements, average toward the value of 500 km sec^{-1} for all CME transients, and with these basic physical parameters Hildner, et al. /30/ estimated that the contribution of material to the total solar wind mass flux by CMEs was less than 4 % of the total during the ATM observing period. A significant result, then, of the critical examination of the time variation of CME production in the ecliptic plane by Hundhausen, et al. /31/ is that the number of CMEs passing the earth per unit time does not seem to vary with the phase of the solar activity cycle. Thus it seems that the incidence of CME generated events found in the solar wind near the earth is nearly constant per unit time. This inferred property of CMEs is an important clue which may be used in the task of identifying the of CME-associated perturbations in the solar wind flux. It is also clear that, unless there is a serious error in either the CME mass estimates or the CME rate, this contribution to the solar wind represents a minor fraction of the total mass flux from the sun over the variation of the solar activity cycle.

Gosling, et al. /47/ identified features in the solar wind where the gradient of the flow velocity was near zero while the density was elevated as "non-compressive density enhancements" (ncde's). Also, the observed proton temperature in these regions is found to be lower. Consistency between the observed frequencies of ncde's and CMEs tends to be the strongest reason for the identification of ncde events as interplanetary consequences of CMEs. MacQueen /9/ pointed out that if it is the case that the magnetic energy content of CMEs is large, as inferred by the association of metric radio emission, an inconsistency is encountered with this identification in that ncde's do not have the enhanced magnetic field strengths implied by metric burst observations.

Another possible candidate for association of CMEs with interplanetary disturbances is the so-called magnetic cloud described by Burlaga, et al. /48/ and Klein and Burlaga /49/. These events exhibit both enhanced magnetic field strength and particle density, and are characterized by a continuous rotation of a component of the interplanetary field as the disturbance passes the detector. Clouds typically are found preceding stream interfaces in the solar wind and tend to follow shocks. In one case, a magnetic cloud has been directly identified with a specific CME by Burlaga, et al. /50/ by using P-78 images of a specific CME event. Using proxy data for the occurrence of CMEs, Wilson and Hildner /51/ found that the evidence linking observed magnetic clouds with CMEs is consistent with the hypothesis of Klein and Burlaga, particularly in cases where type II metric bursts occurred near the central meridian of the sun.

A number of authors have identified interplanetary shocks with CME events. A basic review of the data from which this conclusion is drawn is given by Sheeley, et al. /52/. Using data from the NRL P-78 coronagraph as a source of CME identification and the interplanetary plasma measurements from HELIOS, these authors found that once a shock had been observed at the HELIOS, it was possible to find a corresponding CME event at the sun (within a time window allowed by an assumed range of propagation velocity) in 40 of 80 cases studied. Two problems associated with the identification of an association between interplanetary shocks and CMEs have been encountered in the past. The first of these is the simple observation that the frequency of shocks at 1 A.U. is found to be lower (see MacQueen /9/) than the observed incidence of CMEs. Secondly, the CME mass estimates obtained for near-sun observations of CMEs is about a factor of three smaller than the average mass of an interplanetary shock near the earth (Hundhausen /53/). One possible way in which the difference in mass might be accounted for is to note that most mass estimates of CMEs made near the sun tend to be limited in time between some initial pre-event image and an arbitrary cut-off time selected (usually) by field of view or observing period considerations.

CONCLUDING REMARKS

Tempel's drawing of the 1860 eclipse (Young /54/) shows a coronal structure with the typical arch-like form, although the suggestion that this arch-like structure in an eclipse image might be the effect of a catastrophic ejection of material from the solar corona was not made until about a century later by Eddy /55/. The physical mechanisms required to produce these interesting events still remain obscure, and the inference of the physics of CME production remains a task of high priority for solar and interplanetary physics.

Before the general use of photographic emulsions by astronomers, "nebulae" was a word which was used to lump together all the non-point sources visible in the night sky. Wide use the the photographic plate, and the common use of a taxonomy based on object morphology, quickly resolved this situation. Opposing this experience, the attempt to gain physical insight into the nature of coronal mass ejections has not been served well by published studies of CME morphology. It is possible to make a distinction, at least in the lower corona, between different types of CMEs using speed and acceleration history although the specific physical processes operating at the base of the corona remain obscure. It may be the case that the characteristic response of the media dominates the form and shape of a CME rather than a unique originating process. One could easily think of gas bubbles in a water tank--the cause of the disturbance would be difficult to infer if only the size and speed of the bubble near the top of the tank were available for study.

A number of physical models have been proposed to account for the origin and behavior of CMEs. It is not appropriate to review all, in detail, but a brief review characterizes the diversity of thought on the subject of physical models of CMEs. In general, current models have the following common characteristics: (1) All are forced to include the assumption of an initial magnetic field strength and geometry. (2) All have enough adjustable parameters to reproduce a single characteristic of a CME, namely the magnitude of the speed of the leading edge of the event at the point where acceleration has ceased.

One general type of physical model proposed is that in which CMEs are driven by magnetic forces in a circumstance where the driving mechanism is part of the transient and moves with the disturbance. These so-called magnetically driven transient models neglect interaction with the rest of the corona and do not account for interaction in the atmosphere between the CME and the pre-existing corona. Mouschovias and Poland /56/ invoked magnetic pressure forces

along the loop as a mechanism for driving a CME. Anzer /57/ used the magnetic pressure gradient force generated by an axial current to drive a planar loop. Pneuman /58/ suggested that reconnection occurs near the photosphere, and pre-existing loops are driven outward by an increased magnetic pressure gradient. These three models restricted themselves to loop structures where the line of sight thickness was less than the lateral width of the CME. This leaves open the possibility, neglected to date, that CMEs may be modeled by arcade-like structures driven by magnetic pressure gradient forces.

It has been proposed that CMEs are produced by drivers which are fixed in location at the base of the corona and are physically separate from the CME. The resulting CME is simply a wave-like response to an impulsive pressure input at the interface between the photosphere and corona. This type of mechanism has been used extensively, and is reviewed by, Dryer, et al. /59/. Atmospheric interaction between the transient and corona is considered. This driving mechanism seems to be an attractive one for flare-associated events, but it is difficult to relate an impulsively generated wave model to the kinds of acceleration observed in the slow or epl-associated CME events.

Low /60/ attempted to identify the origin of mass ejection as the consequence of a failure of magnetic tension and gravity forces to constrain expansion by gas and pressure gradient and magnetic pressure gradient forces generated by the evolution of magnetic field regions. The CME originates as an equilibrium state becomes unstable, and by use of a self-similar technique for evaluating the magnetohydrodynamic equations, the evolution of the model transient may be simulated. Low, et al. /61/ have compared results of this technique with a low speed, epl-associated CME seen in the low corona with some success. In that case it was possible to account for the observed variation of CME height-to-width ratio through the lifetime of the event.

The models mentioned above have a common shortcoming. At some point, they fail to account for the totality of the morphological and physical properties observed in CME events. A careful review of the allowable range of model parameters and sensitivity of the results obtained to perturbation would be helpful in the identification of physical effects operating through the lifetime of CME events. For example, it may be the case that more than one originating effect is required for an explanation of the evolution and forms observed in the corona. Key to this effort is a clear statement from the observations concerning the geometrical, morphological, and physical properties of CME events. Particularly, the inference of mass and kinetic energy properties depend upon the determination of the distribution of material in the corona. A more comprehensive analysis of existing data toward a generalized transient geometry now seems to be achievable and is a vital piece of information for future theoretical models.

A second possible approach is the classification of CME events on the basis of event kinematics rather than either morphology. With this in mind, an attempt to find a simple CME classification itself from the observation of CMEs in the lower corona (1.2 - 4.0 $R_\odot$) made with the ATM, SMM coronagraphs, and the K-III coronameter system. This is shown in Table 1; the distinctions being made in terms of kinematic properties and association with other kinds of solar activity. Two broad classes of CME events emerge: The fast CMEs (flare-associated events) which do not appear to be subjected to acceleration above 1.2 $R_\odot$ and the class CME disturbances (epl-associated and slow events) which exhibit clear acceleration between 1.2 and 3.0 $R_\odot$. It is important to remember that the apparent kinematic differences upon which this simple system is based are determined from observations taken in the low corona. A careful implementation of the compressive wave models may, in fact, lead to an explanation of the coronal response of the fast CME events since driving mechanisms are assumed which apply forces at heights below 1.2 $R_\odot$. This is consistent with observed fast transient properties. However, in order to make progress toward understanding the physics of CME transients, a generalized specification of the inferred geometry of accelerated and slow transients is needed from those interpreting observations, so that the correct mass and energy estimates can be supplied to investigators constructing numerical simulations of CME events.

The author gratefully acknowleges the assistance of T. Holzer who carefully read the manuscript and made several helpful and important suggestions. The High Altitude Observatory is a division of the National Center for Atmospheric Research which is operated under the sponsorship of the National Science Foundation.

TABLE 1 Kinematic Classification of CME Events

CME Type	Appearance and Plane-of-the-Sky Velocity ($1.2\text{-}2.2R_\odot$) km sec $^{-1}$	Mass Estimates Grams	Inferred Geometry	Kinetic Energy Estimates ergs	Association With Other Kinds of Solar Activity
CME Events Flare	400-1200 ~ constant velocity from $1.2R_\odot$ upwards	2×10^{14}-2×10^{16} up to ½ of the total mass contributed by the pre-existing corona	Minimum thickness of void = plane-of-the-sky extent, several studies infer bubble shape	10^{+30}-10^{+32}	Flares, Type II metric bursts, long duration x-ray events
EPL CME Events	50-400 Strong acceleration > 50m sec between $1.2\text{-}2.2R_\odot$	2×10^{14}-4×10^{15} Some of the total mass contributed by heating of prominence material	Not comprehensively investigated *	$2\times10^{+28}$-$3\times10^{+30}$	Erruptive prominences (all latitudes)
Slow CME Events	10-50 Nearly constant velocity for many hours with weak acceleration, if any, to heights > $2.2R_\odot$	2×10^{14} from below $1.2R_\odot$, 2×10^{15} from pre-existing corona (single event) *	Not comprehensively investigated *	> $5\times10^{+27}$ - ? *	Active regions, Fe XIV emission regions *

*No comprehensive investigation available.

REFERENCES

1. Hansen, R. T., C. J. Garcia, S. F. Hansen and E. Yasukawa, Abrupt depletions of the inner corona, Pub. Ast. Soc. Pac. 86, 500 (1974)
2. Tousey, R., The solar corona, Space Research 13, 713 (1973)
3. MacQueen, R. M., J. A. Eddy, J. T. Gosling, E. Hildner, R. H. Munro, G. A. Newkirk, Jr., A. I. Poland and C. L. Ross, The outer solar corona as observed from SKYLAB: preliminary results, Astrophys. J. 187, L85 (1974)
4. Fisher, R., R. Lee, R. MacQueen and A. Poland, Mauna Loa coronagraph systems, Appl. Opt. 20, 1094 (1981)
5. Sheeley, N. R., D. J. Michels, R. A. Howard and M. J. Koomen, Initial observations with the SOLWIND coronagraph, Astrophys. J. 257, L99 (1980)
6. MacQueen, R., A. Csoeke-Poeckh, E. Hildner, L. House, R. Reynolds, A. Stanger, H. Tepoel and W. Wagner, The High Altitude Observatory coronagraph polarimeter on the Solar Maximum Mission, Solar Phys. 65, 91 (1980)
7. MacQueen, R. M., Recent interpretation of coronal transient results, Proc. 1983 Solar Physics Workshop, Kunming, Science Press, Beijing, P.R.C., in press (1984)
8. Wagner, W. J., Coronal mass ejections, Ann. Rev. Astron. Ap., in press (1984)
9. MacQueen, R. M., Coronal transients: a summary, Phil. Trans. R. Soc. Lond. A297, 605 (1980)
10. Sheeley, N. R., Jr., R. A. Howard, M. J. Koomen, D. J. Michels, K. L. Harvey and J. W. Harvey, Observations of sunspot structure during sunspot maximum, Space Sci. Rev. 33, 219 (1982)
11. Rock, K. R., R. R. Fisher, C. J. Garcia and E. A. Yasukawa, Summary of Solar Activity Observed at Mauna Loa Solar Observatory: 1980-1983, Technical Note NCAR/TN-221+STR,
12. Jackson, B. V. and E. Hildner, Forerunners: outer rims of solar coronal transients, Solar Phys. 60, 127 (1978)
13. Fisher, R. R. and A. I. Poland, Coronal activity below $2R_\odot$: 1980 February 15-17, Astrophys. J. 246, 1004 (1981)

14. Fisher, R. R., C. J. Garcia and P. Seagraves, On the coronal transient-eruptive prominence of 1980 August 5, Astrophys. J. 246, L161 (1981)

15. Hildner, E., Mass ejections from the solar corona into interplanetary space, in: Study of Traveling Interplanetary Phenomena, ed. M. Shea, D. Smart and S. Wu, D. Reidel, Dordrecht, 1977, p. 3

16. House, L. L., W. J. Wagner, E. Hildner, C. Sawyer and H. U. Schmidt, Studies of the corona with the Solar Maximum Mission coronagraph/polarimeter, Astrophys. J. 244, L117 (1981)

17. Sheeley, N. R., Jr., R. A. Howard, M. J. Koomen and D. J. Michels, Associations between coronal mass ejections and soft x-ray events, Astrophys. J. 272, 349 (1983)

18. Gosling, J. T., E. Hildner, R. M. MacQueen, R. H. Munro, A. I. Poland and C. L. Ross, The speeds of coronal mass ejection events, Solar Phys. 48, 389 (1976)

19. MacQueen, R. M. and R. R. Fisher, The kinematics of solar inner coronal transients, Solar Phys. 89, 89 (1983)

20. Garcia, C., R. Fisher and R. MacQueen, B. A. A. S. 15, #2, 706 (1983)

21. Fisher, R. and C. J. Garcia, Detection of a slowly moving coronal transient event, Astrophys. J. (Letters) in press (1984)

22. Altock, R. and H. Demastus, Coronal transients as observed in Fe XIV 5303A at Sacramento Peak Observatory, B. A. A. S. 15, 706 (1983)

23. Billings, D. E., A Guide to the Solar Corona, Academic Press, New York (1966)

24. Rust, D. M., E. Hildner, M. Dryer, R. T. Hansen, A. W. McClymont, S. M. P. McKenna-Lawlor, D. J. McLean, E. J. Schmahl, R. S. Steinolfson, R. Tandberg-Hanssen, R. Tousey, D. F. Webb and S. T. Wu, Mass ejections, in: Solar Flares, ed. F. Orrall, Colorado Assoc. Univ. Press, 1980, p. 273

25. Van de Hulst, H. C., Electron density of the solar corona, B. A. N. 11, 35 (1950)

26. Fisher, R. and R. H. Munro, Coronal transient geometry: the flare associated transient of 1981 March 25, Astrophys. J. 280, 428 (1984)

27. Crifo, F., J. P. Picat and M. Cailloux, Coronal transients: loop or bubble?, Solar Phys. 83, 143 (1983)

28. Howard, R. A., D. J. Michels, N. R. Sheeley, Jr. and M. J. Koomen, The observations of a coronal transient directed at the earth, Astrophys. J. 263, L101 (1982)

29. Rust, D. M. and E. Hildner, Expansion of an x-ray coronal arch into outer corona, Solar Phys. 48, 381 (1976)

30. Hildner, E., J. Gosling, R. MacQueen, R. Munro, R. A. Poland and C. Ross, Frequency of coronal transients and solar activity, Solar Phys. 48, 127 (1976)

31. Hundhausen, A. J., C. B. Sawyer, L. L. House, R. M. E. Illing and W. J. Wagner, Coronal mass ejections observed during the Solar Maximum Mission: latitude distribution and rate of occurrence, J. Geophys. Res. 86, 2639 (1984)

32. Poland, A. I., R. A. Howard, M. J. Koomen, D. J. Michels and N. R. Sheeley, Jr., Coronal transients near sunspot maximum, Solar Phys. 69, 196 (1982)

33. Munro, R. H., J. T. Gosling, E. Hildner, R. M. MacQueen, A. I. Poland and C. L. Ross, The association of coronal mass ejections with other forms of solar activity, Solar Phys. 61, 201 (1979)

34. Pallavicini, R., S. Serio and G. S. Vaiana, Soft x-ray limb flare images, Astrophys. J. 216, 108 (1977)

35. Fisher, R., Locations of coronal transient sites, B. A. A. S. 15, 70 (1983)

36. Illing, R. M. E. and A. Hundhausen, Possible observation of a disconnected magnetic structure in a coronal transient, J. Geophys. Res. 88, 10210 (1983)

37. Wagner, W. J., SERF studies of mass motions arising in flares, Adv. Space Res. 2, 203 (1983)

38. Gary, D. E., G. A. Dulk, L. L. House, R. Illing, C. Sawyer, W. J. Wagner, D. J. McLean and E. Hildner, Type III bursts, shock waves, and coronal transients: the event of 1980 June 29, 0233 UT, Astron. and Astrophys., in press (1984)

39. Stewart, R. T., G. A. Dulk, K. V. Sheridan, L. L. House, W. J. Wagner, C. Sawyer and R. Illing, Visible light observations of a dense plasmoid associated with a moving Type IV solar radio burst, Astron. and Astrophys. 116, 217 (1982)

40. Gergely, T. E., M. R. Kundu, F. T. Erskine, C. Sawyer, W. J. Wagner, R. Illing, L. L. House, M. K. McCabe, R. T. Stewart, G. J. Nelson, M. J. Koomen, D. Michels, R. Howard and N. Sheeley, Radio and visible light observations of a coronal arcade transient, Solar Phys., in press (1984)

41. Wagner, W. J. and R. M. MacQueen, The excitation of Type II radio bursts in the corona, Astron. and Astrophys. 120, 136 (1983)

42. Wagner, W., Four new insights to coronal mass ejections, Proc. 1984 Solar Physics Workshop, Kunming, Science Press, Beijing, P.R.C., in press (1984)

43. Maxwell, A. and M. Dryer, Characteristics of shocks in the solar corona, as inferred from radio, optical, and theoretical investigations, Space Sci. Rev. 32, 11 (1982)

44. Kahler, S. W., E. W. Cliver, N. R. Sheeley, Jr., R. A. Howard, M. J. Koomen and D. J. Michels, J. Geophys. Res., in press (1984)

45. Sheeley, Jr., N. R., R. J. Steward, R. A. Robinson, M. J. Howard, M. J. Koomen and D. J. Michels, Associations between coronal mass ejections and metric Type II bursts, Ap. J., in press (1984)

46. Cane, H. V., Astron. and Astrophys. in press (1984)

47. Gosling, J., E. Hildner, J. Asbridge, S. Bame and W. Feldman, Noncompressive density enhancements in the solar wind, J. Geophys. Res. 82, 5005 (1977)

48. Burlaga, L., E. Sittler, F. Mariani and R. Schwenn, Magnetic loop behind an interplanetary shock: Voyager, Helios, and IMP 8 observations, J. Geophys. Res. 86, 613 (1981)

49. Klein, L. and L. Burlaga, Interplanetary magnetic clouds at 1 AU, J. Geophys. Res. 87, 8673 (1982)

50. Burlaga, L., L. Klein, N. Sheeley, D. Michels, R. Howard, M. Kooman, R. Schwenn and H. Rosenbauer, A magnetic cloud and a coronal mass ejection, J. Geophys. Res. 9, L1317 (1982)

51. Wilson, R. M. and E. Hildner, Solar Phys., in press (1984)

52. Sheeley, N. R., R. A. Howard, M. J. Koomen, D. J. Michels, R. Schwenn, K. H. Muhlhauser and H. Rosenbauer, Associations between coronal mass ejections and interplanetary shocks, in: Solar Wind Five, NASA CP-2280, 693 (1983)

53. Hundhausen, A. J., Solar Wind and Coronal Expansion, Springer-Verlag, New York, 1972.

54. Young, C. A., The Sun, D. Appleton & Co., New York, 1898.

55. Eddy, J. A., A nineteenth century coronal transient, Astron. Astro. 34, 235 (1974)

56. Mouschovias, T. C. and A. I. Poland, Expansion and broadening of coronal loop transients: a theoretical explanation, Ap. J. 220, 675 (1978)

57. Anzer, U., Can coronal loop transients be driven magnetically, Solar Phys. 57, 111 (1978)

58. Pneuman, G. W., Eruptive prominences and coronal transient, Solar Phys. 65, 369 (1980)

59. Dryer, M., S. T. Wu, R. S. Steinolfson and R. M. Wilson, Magnetohydrodynamic models of coronal transients in the merodinal plane II: simulation of the coronal transient of 1975 Aug. 21, Ap. J. 227, 1059 (1979)

60. Low, B. C., Self-similar magnetohydrodynamics I. The $\gamma = 4/3$ polytrope and the coronal transient, Ap. J. 254, 796 (1982)

61. Low, B. C., R. H. Munro and R. R. Fisher, The initiation of a coronal transient, Ap. J. 254, 335 (1982)